Romanian Reports in Physics, Vol. 65, No. 4, P. 1246–1257, 2013

MOTT SCATTERING IN THE PRESENCE OF AN INTENSE LASER FIELD

MADALINA BOCA

Department of Physics, University of Bucharest, MG-11, Bucharest-Măgurele, 077125 Romania
E-mail: madalina.boca@g.unibuc.ro

Received February 25, 2013

Abstract. We present analytic and numerical results for the scattering of a spin 1/2 particle on a nucleus in the presence of an intense plane-wave laser pulse of arbitrary duration and shape. We obtain the general form of the differential cross section, we describe an approximate method for its numerical evaluation and discuss the general properties of the electron energy and angular distribution. We show that the shape and duration of the laser pulse have a significant influence on the electron distribution. Also a comparison with the results obtained in the monochromatic approximation is included.

PACS: 34.80.Qb, 11.80.-m, 11.55.-m

1. INTRODUCTION

With the recent advent of very powerful laser sources, with intensities up to 10^{22} W/cm^2 already reached [1] or 10^{25} W/cm^2 for envisaged facilities [2], the theoretical interest for the study of fundamental processes in the presence of a laser field increased. Such a process is the laser assisted Mott scattering, which is the subject of this paper. N. F. Mott [3] has studied the process of elastic scattering of an electron in a Coulomb field, using relativistic quantum mechanics. The difference with respect to Rutherford formula is of the order β^2 [4, 5]. Energy is conserved, but not the momentum. In the presence of a monochromatic laser field, the electron energy is not conserved anymore, the scattering being accompanied by the emission or absorption of an arbitrary number of laser photons.

The paper published by Szymanowski *et al.* in 1997 [6] (see also the references therein for a review of previous similar approaches) introduces the formalism for treating the Mott scattering in the presence of a very intense monochromatic laser field. The electron dressed by the laser is described by a Volkov solution [7] and the interaction with the Coulomb potential is described in the first order perturbation theory (first Born approximation). The same method was used also for treating other laser-assisted processes, as non-linear Compton scattering, laser assisted Bremsstrahlung, Møller scattering, or more recently, pair creation in the presence of a very intense laser field. For a review of the literature see [8, 9].

In the cited paper, Szymanowski and coworkers present numerical and analy-

tical results concerning relativistic and spin effects for a circularly polarized laser field. Mott scattering of a Klein-Gordon particle was studied in [10]. Spin effects, calculated in the same formalism, are presented in [11–14] for linearly polarized monochromatic laser field and in [15] for elliptic polarization. Li *et al.* [16] studied the Mott scattering beyond the Born approximation, by using relativistic Coulomb-Volkov electronic states; they studied the influence of the Coulomb distortion of the electron motion for moderate laser intensity.

The electron energy spectrum calculated in the framework of monochromatic approximation consists in an infinite series of discrete values, dependent on the observation direction. The purpose of this paper is to go beyond the monochromatic approximation for the laser field, considering a finite plane wave laser pulse; we shall see that in this case the spectrum becomes continuous. Our formalism allows us to consider very intense plane wave laser pulse, with fixed propagation direction but arbitrary duration and shape. We show that the finite duration and also the shape of the laser pulse influence the scattered electron distribution. The method is similar to that used previously for the study of non-linear Compton scattering in the presence of an intense laser pulse [17], [18]. The electronic states are described by Volkov solutions in a laser pulse; the interaction with the Coulomb potential is treated in the first order perturbation theory, as in [6], [11–14]. Neglecting the higher order effects of the potential is justified for the case of relativistic electrons, and very high laser intensity, considered in our numerical examples.

In Sect. 2 we present the expression of the transition amplitude of the process and the differential cross section in the case when the initial electron beam is unpolarized and the spin in the final state is not detected. In Sect. 3 we discuss the numerical method for evaluation of the differential cross section and present examples of numerical results. We also discuss the general properties of the electron distributions and the effects of the laser pulse shape and duration.

2. THE TRANSITION AMPLITUDE AND THE DIFFERENTIAL CROSS SECTION

We start from the Dirac equation for a charged particle in the presence of the external field described by the vector potential A_t, $[\gamma_\mu(P^\mu - eA_t^\mu) - mc]\,\Psi = 0$; here γ_μ are the well known Dirac matrices, P^μ the components of the four-momentum operator $P^\mu = \mathrm{i}\hbar\partial^\mu$. In the case of laser assisted Mott scattering the external field has two components: the Coulomb potential of the fixed nucleus and the laser field. Then the total vector potential A_t is the sum of two terms $A_t = A_C + A_L$; A_C is the vector potential describing the interaction of the electron with a nucleus of charge $Z|e|$ and A_L the vector potential of a laser field whose propagation direction will be denoted by $\mathbf{n}$. In the following we shall take the z direction of the coordinate frame

along $\mathbf{n}$. In order to describe a plane-wave field we must choose A_L as a function depending on time and coordinates only through the combination $\phi = ct - \mathbf{n}\cdot\mathbf{r}$. We introduce the four vector $n \equiv (1, \mathbf{n})$; the argument of the laser vector potential can be written as $\phi = ct - \mathbf{n}\cdot\mathbf{r} \equiv n \cdot x$ and the Lorentz gauge condition $\partial_\mu A_L^\mu = 0$ becomes $n \cdot A_L = 0$. Then a possible choice for A_L is $A_L(\phi) :\equiv (0; \mathbf{A}(\phi))$, with $\mathbf{A}(\phi)\cdot\mathbf{n} = 0$. Next we use the standard method of perturbation theory, by splitting the Hamiltonian in two parts: the unperturbed Hamiltonian H_0, which describes the electron in the laser field, and the interaction with the Coulomb potential, treated as a perturbation $H_{int} = -Ze_0^2/|\mathbf{r}|$, where $e_0^2 = e^2/(4\pi\epsilon_0)$. Because we consider the case of a laser pulse with finite duration, such that $\lim_{t\to\pm\infty} A_L = 0$, we can take the initial and final states (at $t \to -\infty$ and respectively $t \to \infty$) of the electron as free states of momenta p_1 and p_2, denoted by $|\phi_{i_1}(p_1; t)\rangle$ and $|\phi_{i_2}(p_2; t)\rangle$ where i_1 and i_2 are the initial and respectively final spin indices and

$$\phi_i(p; x) = \frac{1}{\sqrt{V}} e^{-ip\cdot x}\xi_i(p) \tag{1}$$

with $\xi_i(p)$ the free Dirac spinors, solutions of the equation $(\gamma_\mu p^\mu - mc)\xi_i(p)$. We emphasize that this approach is possible because, unlike in the monochromatic approximation, we consider here finite laser pulses. In the presence of the laser field, at finite times t, the free states become Volkov states [7], solutions of the Dirac equation for the electron in a plane wave electromagnetic field $A_L(\phi)$. If we denote by U_0 the evolution operator associated to the Hamiltonian of the electron in the laser field H_0 we have

$$U_0(t, -\infty)|\phi_{i_1}(p_1; -\infty)\rangle = |\psi_{i_1}(p_1; t)\rangle, \quad \langle\phi_{i_2}(p_2; \infty)|U_0(\infty, t) = \langle\psi_{i_2}(p_2; t)|$$

where $|\psi_i(p; t)\rangle$ are Volkov solutions in a laser *pulse*, originating from free plane waves. As a consequence the transition amplitude in the first order perturbation theory with respect to the interaction Hamiltonian H_{int} becomes

$$\mathcal{A}(p_1, i_1; p_2, i_2) = \frac{-Ze^2}{i\hbar}\int_{-\infty}^{\infty} dt \int d\mathbf{r}\psi_{i_2}^\dagger(p_2; \mathbf{r}, t)\frac{1}{|\mathbf{r}|}\psi_{i_1}(p_1; \mathbf{r}, t). \tag{2}$$

Next, the calculation is similar to that in the monochromatic approximation: we introduce in the expression of the transition amplitude the Volkov solutions for a laser pulse (see, for example [18]) and express the Coulomb potential by its Fourier transform

$$\frac{1}{|\mathbf{r}|} = \frac{1}{(2\pi)^{3/2}}\int d\mathbf{q} e^{i\mathbf{q}\cdot\mathbf{r}} V(\mathbf{q}), \quad V(\mathbf{q}) = \frac{2}{(2\pi)^{1/2}}\frac{1}{|\mathbf{q}|^2}. \tag{3}$$

Then we obtain we obtain the transition amplitude expressed as a seven-dimensional integral; in order to calculate it, we perform first a change of variable in the spatio-

temporal integral $\{\mathbf{r},t\} \longrightarrow \{\mathbf{r}_\perp, \phi = ct - \mathbf{n}\cdot\mathbf{r}, \widetilde{\phi} = ct + \mathbf{n}\cdot\mathbf{r}\}$, where the index $\perp$ indicates the components orthogonal on the unity vector $\mathbf{n}$ of the laser propagation direction. The integrals over $\mathbf{r}_\perp$ and $\widetilde{\phi}$ can be calculated directly, leading to $\delta(\mathbf{p}_{1\perp} - \mathbf{p}_{2\perp} + \hbar\mathbf{q}_\perp) \times \delta(n\cdot p_1 - n\cdot p_2 + \hbar\mathbf{n}\cdot\mathbf{q})$. In the next step the δ functions are used to eliminate the three integral over $\mathbf{q}$, and finally the transition amplitude becomes

$$\mathcal{A}(p_1,i_1;p_2,i_2) = -\frac{1}{V}\frac{Ze^2}{i\hbar c}\frac{4\pi\hbar^2}{(\mathbf{p}_{1\perp}-\mathbf{p}_{2\perp})^2 + (n\cdot p_1 - n\cdot p_2)^2}\langle p_2 i_2|\mathcal{Q}|p_1 i_1\rangle \quad (4)$$

where the matrix $\mathcal{Q}$ is a sum of four terms

$$\mathcal{Q} = b_2\frac{(mc)^2}{2(n\cdot p_1)(n\cdot p_2)}\hat{n} + b_0\gamma_0 + \frac{mc}{2n\cdot p_1}\gamma_0\hat{a}\hat{n} + \frac{mc}{2n\cdot p_2}\hat{n}\hat{a}\gamma_0. \quad (5)$$

In the previous equations the "Feynman slash" was denoted by $\hat{v} \equiv \gamma_\mu v^\mu$ and four integrals over the remaining variable ϕ were introduced:

$$\mathbf{a} = \int_{-\infty}^{\infty} d\phi \frac{-e\mathbf{A}(\phi)}{mc}\exp[-\frac{i}{\hbar}G(\phi)], \quad a \equiv (0,\mathbf{a}), \quad (6)$$

$$b_0 = \int_{-\infty}^{\infty} d\phi \exp[-\frac{i}{\hbar}G(\phi)], \quad b_2 = \int_{-\infty}^{\infty} d\phi \frac{e^2A^2(\phi)}{(mc)^2}\exp[-\frac{i}{\hbar}G(\phi)], \quad (7)$$

with

$$G(\phi) = \phi(p_1^0 - p_2^0) + F(\phi,p_1) - F(\phi,p_2) \quad (8)$$

and

$$F(\phi,p) = \frac{1}{2n\cdot p}\int^{\phi} d\chi \frac{e^2A^2(\chi)}{(mc)^2} + \frac{\mathbf{p}}{n\cdot p}\cdot\int^{\phi} d\chi\frac{-e\mathbf{A}(\chi)}{(mc)}. \quad (9)$$

In the case of zero field intensity $\mathbf{a}$ and b_2 vanish, b_0 reduces to $2\pi\hbar c\delta(E_1 - E_2)$ and we re-obtain the well known amplitude of the Mott scattering (see, for example, [5], §7.1) and the conservation rule of the energy $E_1 = E_2$. If a laser pulse of finite duration $\lim_{\phi\to\pm\infty} A(\phi) = 0$ is present, the integrals a_x, a_y and b_2 are finite and non-zero for any final energy E_2; the integral b_0 is discussed in Appendix A. Its expression is given in Eq. (19); it contains a term proportional with $\delta(E_1 - E_2)$, as in the field-free case, and a part linear in $\mathbf{a}$ and b_2.

From the previous results one can see that, unlike in the field-free case, the scattered electron has a continuous energy spectrum, taking any value between mc^2 and infinity. However, in Sect. 3 we show that for given initial electron energy and direction and laser pulse parameters the energy distribution of the final electron has non-negligible values only for E_2 in certain intervals, which can be obtained as solutions of a simple equation.

The differential cross section is obtained by the standard method: the modulus square of the transition amplitude is multiplied by the elementary volume in the final state space $Vd\mathbf{p}_2/(2\pi\hbar)^{3/2}$ and divided by the flux of the initial electron $J_{inc} = |\mathbf{v}_1|/V$ and by the duration of the laser pulse. Here we present the results for the case of unpolarized beams of electrons; the result is obtained by taking the average/sum over the initial/final electron spin.

$$d\sigma = Z^2 r_0^2 \frac{1}{c^2\tau\pi\hbar} \frac{(mc)^4}{[(\mathbf{p}_{1\perp} - \mathbf{p}_{2\perp})^2 + (n\cdot p_1 - n\cdot p_2)^2]^2} R dE_2 d\Omega_2 \tag{10}$$

with r_0 the classical electron radius and

$$\begin{aligned} R = {} & |b_0|^2 \left[1 + \frac{p_1^0 p_2^0 + \mathbf{p}_1\cdot\mathbf{p}_2}{(mc)^2}\right] + |b_2|^2 \frac{(mc)^2}{2(n\cdot p_1)(n\cdot p_2)} + |\mathbf{a}|^2 \frac{p_1\cdot p_2 - (mc)^2}{(n\cdot p_1)(n\cdot p_2)} \\ & + \frac{(mc)^2}{(n\cdot p_1)(n\cdot p_2)} \Re\left\{ b_2^* \left[b_0 + \mathbf{a}\cdot\frac{\mathbf{p}_1 + \mathbf{p}_2}{mc}\right]\right\} + \frac{2}{(n\cdot p_1)(n\cdot p_2)} \Re\{(\mathbf{a}\cdot\mathbf{p}_1)(\mathbf{a}^*\cdot\mathbf{p}_2)\} \\ & + \frac{1}{mc}\Re\left\{ b_0^* \left[\mathbf{a}(\cdot\mathbf{p}_1 + \mathbf{p}_2) + \mathbf{a}\cdot\left(\mathbf{p}_1 \frac{p_2^0 + \mathbf{n}\cdot\mathbf{p}_2}{n\cdot p_1} + \mathbf{p}_2 \frac{p_1^0 + \mathbf{n}\cdot\mathbf{p}_1}{n\cdot p_2}\right)\right]\right\}. \end{aligned} \tag{11}$$

The differential cross section is singular for $\mathbf{p}_1 = \mathbf{p}_2$ due to the factor in front of R in Eq. (10), also, for $E_1 = E_2$, even at different directions of the initial and final electron, it is singular because of the integral b_0. In the next section we discuss the numerical method for evaluation of $d\sigma/dE_2 d\Omega_2$ and numerical results.

3. NUMERICAL METHOD AND RESULTS

We shall present results for the double differential cross section $\frac{d\sigma}{dE_2 d\Omega_2}$, calculated according to Eq. (10) for $E_2 \neq E_1$; for $E_1 = E_2$ the result is singular. Everywhere in this section we consider the nucleus charge $Z = 1$. For $E_1 \neq E_2$ the expression (19) of b_0 becomes

$$b_0 = \frac{1}{p_1^0 - p_2^0}\left[-(mc)\mathbf{a}\cdot\left(\frac{\mathbf{p}_1}{n\cdot p_1} - \frac{\mathbf{p}_2}{n\cdot p_2}\right) - \frac{(mc)^2}{2} b_2 \left(\frac{1}{n\cdot p_1} - \frac{1}{n\cdot p_2}\right)\right]. \tag{12}$$

The numerical problem reduces to the calculation of integrals of the form

$$\mathcal{I} = \int_{-\infty}^{\infty} d\phi h(\phi) \exp\left[-\frac{i}{\hbar} G(\phi)\right] \tag{13}$$

with $G(\phi)$ defined in (8), $h(\phi)$ being (up to a factor) either a component of the laser field vector potential (for the integrals a_x, a_y), either its square (for b_2). For the laser

pulse we choose a $\sin^2$ shape and circular polarization

$$\mathbf{A}(\phi) = \frac{A_0}{\sqrt{2}} f(\phi) \left[\mathbf{e}_x \cos(k\phi) + \mathbf{e}_y \sin(k\phi)\right], \quad f(\phi) = \sin^2\left(\frac{k\phi}{2N_t}\right) \tag{14}$$

of central frequency $\omega = k/c$, and length $\tau = 2N_t$ cycles. We use the dimensionless parameter $\eta = |e|A_0/(mc)$ in order to characterize the laser intensity.

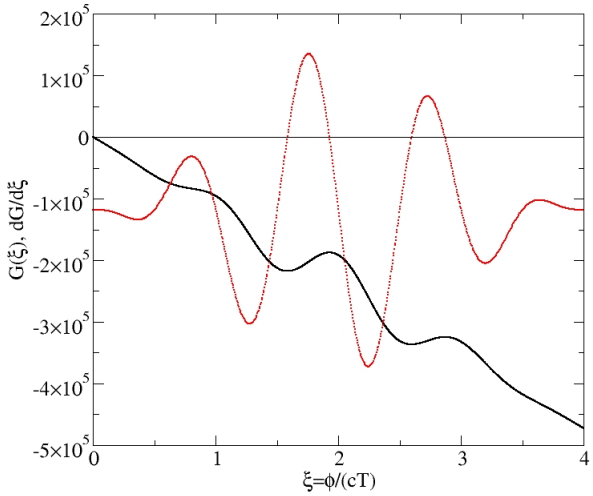

Fig. 1 – The function $G(\xi \equiv \phi/ct)$ (full black line) and its derivative $dG/d\xi$ (dotted red line) for the parameters presented in text.

The main difficulty in the evaluation of the integrals $\mathcal{I}$ appears because the exponent $G(\phi)$ changes rapidly with ϕ, which makes the integrand very fast oscillating. As an example, we present in Fig. 1 a graphic of $G(\phi)$ for a typical case: the laser pulse has the central frequency $\omega_0 = 0.05$ a.u. and $\eta = 1$; the initial electron has the Lorentz factor $\gamma_1 = 10$, and its momentum is directed in the negative sense of the z axis (*i.e.* counter propagating with respect to the laser pulse). For the final electron we choose $\gamma_2 = 10.05$ and its direction is characterized by the polar angles $\theta = 0.9\pi$, $\phi = 0$ (*i.e.* the angle between the initial and final direction of the electron $\Delta\theta = 0.1\pi$). In Fig. 1 is represented with full (black) line the graphic of G, as argument we have chosen the scaled parameter $\xi = \phi/(cT)$, which varies in the interval $(0, 4)$ for a pulse with $N_t = 4$ cycles. Also with dotted (red) line is represented the derivative of G with respect to ξ.

The integrals $\mathcal{I}$ can be calculated with very good precision by direct methods, *e.g.* by the trapezoidal rule, but this approach is very time consuming; beside this direct calculation, which will be named in the following "exact calculation of the integrals", we have tested the stationary phase approximation for evaluating the same

integrals, according to which

$$\int_{-\infty}^{\infty} d\phi h(\phi) \exp\left[-\frac{i}{\hbar}G(\phi)\right] \approx \sum_i \sqrt{\frac{2\pi}{i|G''(\phi_i)|}} h(\phi_i) \exp\left[-\frac{i}{\hbar}G(\phi_i)\right]. \qquad (15)$$

where ϕ_i are the zeros of the derivative of $G(\phi)$; in the example presented previously there are four zeros of $G'(\phi)$. In this approximation an integral $\mathcal{I}$ is non-zero if there is at at least one real zero of $G'(\phi)$. To illustrate the precision of the method we present in Fig. 2 (a) a graph of the double differential electron distribution $d^2\sigma/dE_2 d\Omega_2$ as a function of the energy of the final electron; the parameters of the laser pulse and of the incident electron are the same as those used in Fig. 1, also the direction of the final electron is fixed, as previously. The variable on the abscissa is the difference $\Delta\gamma = \gamma_1 - \gamma_2$ between the Lorentz factors of the the initial and final electron.

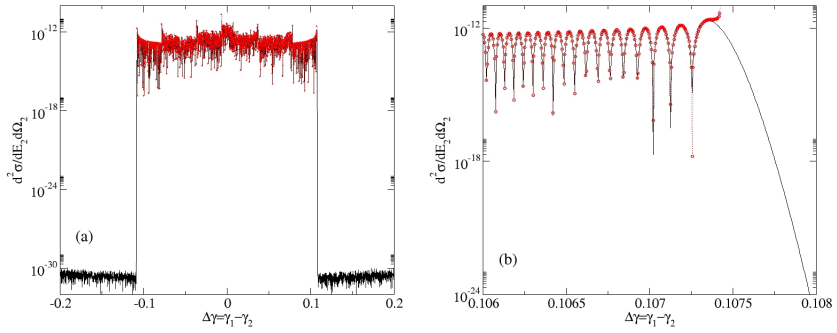

Fig. 2 – (a): The double differential electron cross section $d^2\sigma/dE_2 d\Omega_2$ as a function of the final electron energy, for the conditions mentioned in text; full (black) line: exact calculation, circles (red) approximate calculation. (b): detail of (a).

One can see that the exact results (represented with full black line) take considerable larger values in the domain $|\Delta\gamma| \lesssim 0.11$ than for $|\Delta\gamma| \gtrsim 0.11$. In the last case the exact results show an abrupt decrease, with almost 20 orders of magnitude. The approximate results, presented with red circles, are very close to the exact ones in the first domain and vanish in the second domain (this is because for $|\Delta\gamma| \gtrsim 0.11$ the derivative of $G(\phi)$ has no real zeros *). In Fig. 2 (b) we present a detail of Fig. 2 (a) for a very small range of $\Delta\gamma$ close to the right limit of the region with practically non-vanishing values; here it is clear the very good agreement between exact and approximate values.

*In the region where $G'(\phi)$ has no real zeros one can try to extend the numerical method looking for zeros in the complex plane; in this case one obtains a non-zero approximate result even in the second domain. As in this case the results are extremely small, close to the exact ones, we ignore them.

Next we discuss the shape of the differential cross section as displayed in Fig. 2; one can see clearly a "ladder-like structure" with well defined successive steps, approximately symmetric with respect to $\Delta\gamma = 0$ and decreasing from the "center" ($\Delta\gamma = 0$) towards the edges. In our example, the highest "step" ranges in the interval $|\Delta\gamma| \lesssim 0.007$, the next steps, to the left and right of the central one, are located in the interval $0.007 \lesssim |\Delta\gamma| \lesssim 0.036$, the next one lies in $0.036 < |\Delta\gamma| \lesssim 0.079$ and the last "steps" are in the region $0.079 < |\Delta\gamma| \lesssim 0.108$. The origin of this structure can be understood also in the frame of the approximate method of calculation we use: we have checked that in the first interval there are 8 zeros of $G'(\phi)$ contributing to the integrals (13), in the second interval only 6 zeroes contribute, and so on. Obviously, for the case of a long laser pulse, the successive steps become sharper and their number increases, and in the end the structure is "smeared". We mention that the symmetry of the distribution with respect to $\Delta\gamma = 0$ is only approximative, and it disappears when the laser intensity increases, as we shall see in the following.

In the following we study in more detail the electron distribution; as we consider only the case of head-on collision and circular polarization of the laser, the distributions will be symmetric with respect to the angle ϕ_2. We present in Fig. 3 the energy angular distribution $d^2\sigma/dE_2 d\Omega_2$ in a logarithmic colour map. The initial electron parameters and the laser pulse shape and central frequency are those already mentioned. The laser intensity changes: we have $\eta = 1$ in (a), $\eta = 2$ in (b), $\eta = 5$ in (c) and $\eta = 10$ in (d). The calculation is performed using the approximation mentioned

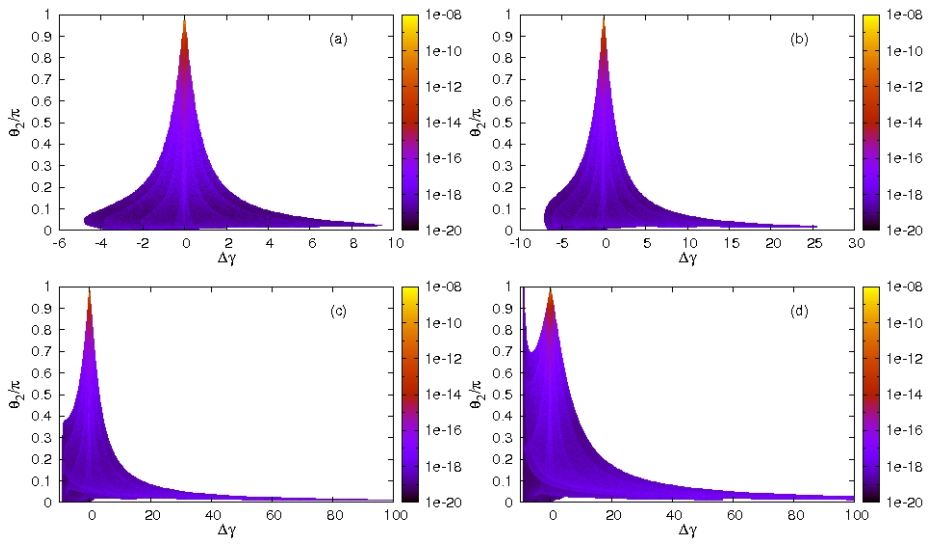

Fig. 3 – The energy angular distribution $d^2\sigma/dE_2 d\Omega_2$ in a logarithmic colour map; (a) $\eta = 1$, (b): $\eta = 2$, (c): $\eta = 5$, (d): $\eta = 10$.

before; the region in the plane $(\gamma_2 - \theta_2)$ in which the results are zero is represented in white. If we used the exact calculation of the integrals $\mathcal{J}$, the zeroes in the white region would be replaced by very small values, negligible with respect to those represented. We can see that the electron distribution has a very sharp peak close to the initial electron direction ($\theta_1 = \pi$), but it is non-zero for very large domains in energy, especially for small values of θ_2, and the domain of non vanishing probabilities extends very fast when η increases [†]. It is also worth noting that the number N of photons involved in the process is extremely large even for small field intensity; for example, a change of the Lorentz factor of the electron $\Delta\gamma = 1$ is realized by absorption of $N \sim 10^5$ photons of energy $\hbar\omega = 0.05$ a.u. (1.36 eV).

The limits of region in which the electron distribution is non-negligible can be obtained easily in the framework of the approximation we use, by imposing the condition that the derivative of the phase in the integrand of $\mathcal{I}$ has at least a real zero. This condition leads to a domain of possible energies and directions of the final electron. If we consider the case of a rectangular pulse, for which the envelope of $\mathbf{A}$ is, or can be approximated as, constant, this condition becomes very simple. For, example, for circular polarization $G'(\phi)$ has the expression

$$\frac{dG}{d\phi} = q_1^0 - q_2^0 + \frac{\hbar\omega}{c}\Delta_0 \cos(k\phi - d) \tag{16}$$

where q_1^0, q_2^0 are the temporal components of the dressed initial and respectively final electron momenta, defined as $q_i^0 = p_i^0 + \frac{e^2 A_0^2}{2n\cdot p_i}$, $\quad i = 1, 2$ and

$$d = \arctan\frac{\delta_y}{\delta_x}, \quad \Delta_0 = \frac{\delta_x}{d}, \qquad \delta_i = \frac{-ecA_0}{\hbar\omega}\left(\frac{p_{1i}}{n\cdot p_1} - \frac{p_{2i}}{n\cdot p_2}\right), \quad i = x, y. \tag{17}$$

$G'(\phi)$ has at least a real zero if

$$\frac{c|q_1^0 - q_2^0|}{\hbar\omega|\Delta_0|} \leq 0; \tag{18}$$

for fixed initial conditions and fixed direction of the final electron, this condition gives an equation for the possible values of the energy of the final electron.

The same condition can be re-obtained in the monochromatic limit. In this case the transition amplitude is expressed as an infinite series of Bessel functions $J_N(\Delta_0)$ [6], each term being multiplied by $\delta(E_{q_1} = E_{q_2} + N\hbar\omega)$. The δ functions in the monochromatic limit expresses the energy conservation relation: the difference between the energies $E_{q_1} = cq_1^0$ and $E_{q_2} = cq_2^0$ of the *dressed* initial and final electron must be a multiple of the laser field frequency ω. A limit of the maximum number of photons contributing to the cross section can be found from the asymptotic expres-

[†]Note, however, that the region $\Delta\gamma < 0$ it is naturally limited to $\Delta\gamma = -9$, since this corresponds to the final electron at rest.

sion of the Bessel functions for large order [19] $J_N(z) \sim \frac{1}{\sqrt{2\pi N}} \left(\frac{ez}{2N}\right)^N, \quad N \gg 1$ from the above it follows that the Bessel functions (and in consequence the transition amplitude) decrease fast if $|z| \geq N$. In our case, the condition $|\Delta_0| \leq |N_{max}|$ an be written also, using the conservation relation imposed by the δ function, as $\hbar\omega|\Delta_0| \leq |E_{q_1} - E_{q_2}|$ which is identical with the condition (18).

As an example, in Fig. 4 we study the electron distribution for different pulse shapes. As before, the polarization is circular, $\eta = 10$, the initial electron energy is $E_1 = 10mc^2$. In Fig. 4 (a), (b), (c) we considered a pulse of $\sin^2$ shape, given in Eq. (14), of length $\tau = 1$ cycle, respectively 20 cycles and 50 cycles. One can see that when the pulse length increases from one cycle to twenty, there are important differences between the corresponding distribution shapes. On the other hand, further increase of the pulse length at constant shape, *e.g.* to 50 cycles does not changes the distribution any more, as the difference between the cases (b) and (c) is practically negligible. In Fig. 4 (d) we considered the case of a rectangular pulse, with constant amplitude and duration of 50 cycles; this case is in fact identical with the case of a monochromatic pulse. Now, the distribution for $\Delta\gamma > 0$ is similar to that obtained for a $\sin^2$ pulse of equal length (Fig. 4 (c)). However, for $\Delta\gamma < 0$ there are differences between the two cases, the allowed domain being smaller for the rectangular pulse. In conclusion, we have shown that not only the length but also the shape of the laser field can influence significantly the shape of the final electron distribution.

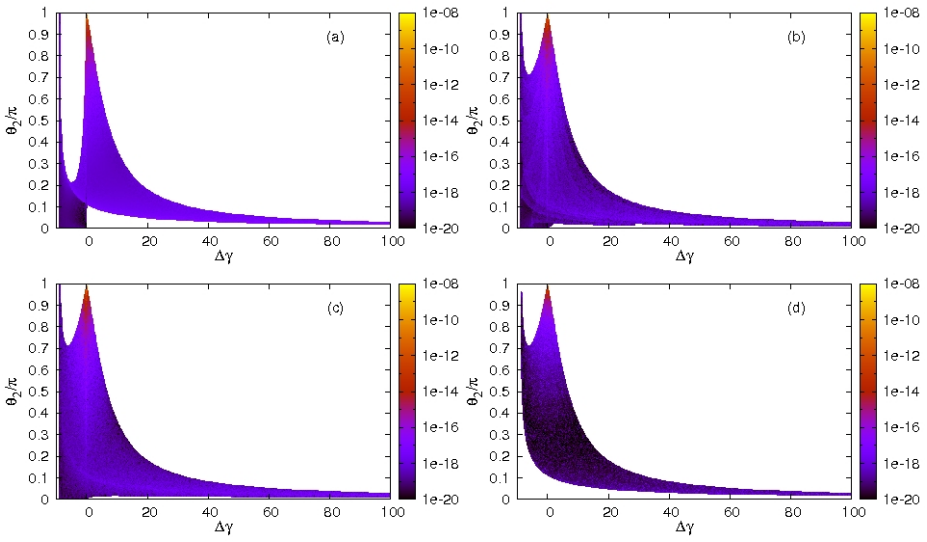

Fig. 4 – The energy angular distribution $d^2\sigma/dE_2 d\Omega_2$ in a logarithmic colour map; (a): $\sin^2$ pulse with $\tau = 1$ cy, (b): $\sin^2$ pulse with $\tau = 20$ cy, (c): $\sin^2$ pulse with $\tau = 50$ cy, (d): rectangular pulse with $\tau = 50$ cy.

A. THE RELATION BETWEEN THE INTEGRALS a, b_2 AND b_0

We start our analysis by observing that the integral b_0 is divergent; for regularization we introduce a convergence factor, and define $b_0 = \lim_{\epsilon\to 0_+} b_0(\epsilon)$ with

$$b_0(\epsilon) = I_- + I_+, \quad I_\pm = \pm \int_0^{\pm\infty} d\phi \exp[-\frac{i}{\hbar}(\phi(p_1^0 - p_2^0 \mp \hbar\epsilon) + F(\phi, p_1) - F(\phi, p_2))].$$

Next, each of the two integrals above can be integrated by parts and, by taking the limit $\epsilon \to 0_+$ one finds

$$b_0 = \pi\hbar\delta(p_1^0 - p_2^0)\left[e^{-\frac{i}{\hbar}G(\infty)} + e^{-\frac{i}{\hbar}G(-\infty)}\right] - \frac{\mathcal{P}}{p_1^0 - p_2^0}\int_{-\infty}^{\infty} d\phi \frac{dG(\phi)}{d\phi} e^{-\frac{i}{\hbar}\phi(p_1^0 - p_2^0) + G(\phi)}$$

with $\mathcal{P}$ the principal part. If we express the remaining convergent integral in terms of $\mathbf{a}$ and b_2 we have

$$b_0 = \pi\hbar\delta(p_1^0 - p_2^0)\left[\exp(-\frac{i}{\hbar}G(\infty)) + \exp(-\frac{i}{\hbar}G(-\infty))\right]$$
$$+ \mathcal{P}\frac{1}{p_1^0 - p_2^0}\left[-(mc)\mathbf{a}\cdot\left(\frac{\mathbf{p}_1}{n\cdot p_1} - \frac{\mathbf{p}_2}{n\cdot p_2}\right) - \frac{(mc)^2}{2} b_2\left(\frac{1}{n\cdot p_1} - \frac{1}{n\cdot p_2}\right)\right]. \quad (19)$$

It is worth noting here that Eq. (19) is a generalization of the similar relation met in the case of Compton scattering (see [17], Eq. (25), (26), (31)).

Acknowledgements. This work was supported by the strategic grant POSDRU/89/1.5/S/58852, Project "Postdoctoral programme for training scientific researchers" co-financed by the European Social Found within the Sectorial Operational Program Human Resources Development 2007-2013. The author is grateful to Viorica Florescu and Virgil Baran for useful discussions and constant encouragement.

REFERENCES

1. V. Yanovsky *et al.*, Opt. Express **16**, 2109 (2008).
2. `http://www.extreme-light-infrastructure.eu/`.
3. N.F. Mott, Proc. R. Soc. London Ser. A **124**, 425 (1929); **135**, 429 (1932).
4. W.A. McKinley and H. Feshbach, Phys. Rev. **74**, 1739 (1948).
5. J.D. Bjorken and S.D. Drell, *Relativistic quantum mechanics* (McGraw-Hill, 1964).
6. C. Szymanowski *et al.*, Phys. Rev. A **56**, 3846 (1997).
7. D.M. Volkov, Z. Physik **94**, 250 (1935).
8. F. Ehlotzky , K. Krajewska and J.Z. Kaminski, Rep. Prog. Phys. **72**, 046401 (2008).
9. A. Di Piazza *et al.*, Rev. Mod. Phys **84**, 1177 (2012).
10. J.Z. Kaminski and F. Ehlotzky, Phys. Rev. A **59**, 2105 (1999).

11. P. Panek, J.Z. Kaminski and F. Ehlotzky, Phys. Rev. A **65**, 033408 (2002).
12. M.W. Walser *et al.*, Phys. Rev. A **65**, 043410 (2002).
13. S.M. Li, J. Berakdar, J. Chen, Z.F. Zhou, Phys. Rev. A **67**, 063409 (2003).
14. B. Manaut, S. Taj and Y. Attaourti, Phys. Rev. A **71**, 043401 (2005).
15. P. Panek, J.Z. Kaminski, and F. Ehlotzky, Laser Phys. **13**, 1399 (2003).
16. S.M. Li, J. Berakdar, J. Chen, Z.F. Zhou, J. Phys. B **37**, 653 (2004).
17. M. Boca and V. Florescu, Phys. Rev. A **80**, 053403 (2009).
18. M. Boca, V. Dinu and V. Florescu, Phys. Rev. A **86**, 013414 (2012).
19. Milton Abramowitz, Irene A. Stegun, *Handbook of Mathematical Functions* (Courier Dover Publications, 1964).